



**HAL**  
open science

## Crystal structure and magnetism of MnO under pressure

S. Klotz, K. Komatsu, A. Polian, S. Machida, A. Sano-Furukawa, J.-P. Itié, T. Hattori

► **To cite this version:**

S. Klotz, K. Komatsu, A. Polian, S. Machida, A. Sano-Furukawa, et al.. Crystal structure and magnetism of MnO under pressure. *Physical Review B: Condensed Matter and Materials Physics* (1998-2015), 2020, 101. hal-02506986

**HAL Id: hal-02506986**

**<https://hal.sorbonne-universite.fr/hal-02506986>**

Submitted on 12 Mar 2020

**HAL** is a multi-disciplinary open access archive for the deposit and dissemination of scientific research documents, whether they are published or not. The documents may come from teaching and research institutions in France or abroad, or from public or private research centers.

L'archive ouverte pluridisciplinaire **HAL**, est destinée au dépôt et à la diffusion de documents scientifiques de niveau recherche, publiés ou non, émanant des établissements d'enseignement et de recherche français ou étrangers, des laboratoires publics ou privés.

## Crystal structure and magnetism of MnO under pressure

S. Klotz,<sup>1</sup> K. Komatsu,<sup>2</sup> A. Polian,<sup>1</sup> S. Machida,<sup>3</sup> A. Sano-Furukawa,<sup>4</sup> J.-P. Itié,<sup>5</sup> and T. Hattori<sup>4</sup>

<sup>1</sup>*IMPMC, CNRS UMR 7590, Sorbonne Université, 4 Place Jussieu, F-75252 Paris, France\**

<sup>2</sup>*Geochemical Research Center, Graduate School of Science,*

*The University of Tokyo, 7-3-1 Hongo, Bunkyo-ku, Tokyo 113-0033, Japan*

<sup>3</sup>*CROSS, Neutron Science and Technology Center, 162-1 Shirakata, Tokai, Ibaraki 319-1106, Japan*

<sup>4</sup>*J-PARC Center, Japan Atomic Energy Agency, 2-4 Shirakata, Tokai, Ibaraki 319-1195, Japan*

<sup>5</sup>*Synchrotron SOLEIL, Saint Aubin BP 48, 91192 Gif sur Yvette Cedex, France*

(Dated: February 28, 2020)

Manganese oxide is a prototype of an antiferromagnetic Mott-insulator. Here we investigate the interplay of magnetic ordering and lattice distortion across the Néel temperature  $T_N$  under pressure using neutron and x-ray diffraction. We find an increase of  $T_N$  with a rate of  $dT_N/dP=+4.5(5)$  K/GPa, an increase of the rhombohedral distortion  $\alpha$  by  $d\alpha/dP=+0.018$  deg./GPa, as well as a volume striction which is insensitive to pressure. These results allow retrieving the dependence of the coupling constants  $J_1$  and  $J_2$  on interatomic distances and compare it to first-principles predictions. Antiferromagnetic diffuse scattering was observed up to  $\approx 1.2 T_N$ , and long-range magnetic order appears at room temperature at 42 GPa.

### INTRODUCTION

Manganese oxide (MnO) is a representative of the archetypal 3d-monoxide series which have been investigated since decades being textbook examples of highly correlated electron systems. At ambient conditions it is a paramagnetic Mott-insulator crystallizing in an face-centred cubic (fcc) structure. Similar to NiO, CoO, and FeO type-II antiferromagnetic order occurs below the Néel temperature ( $T_N = 120$  K for MnO), accompanied by a small rhombohedral distortion. Recent interest in MnO under pressure was mostly motivated by the search for a Mott transition in MnO under strong compression: X-ray and resistivity measurements up to Mbar pressures report a collapse of the magnetic moment starting at 60 GPa and followed by metallisation between 90 and 105 GPa [1–4].

Beyond the focus on Mott or high-to-low-spin transitions, surprisingly less is known about structural and magnetic parameters in the intermediate 0-10 GPa range where the fcc/rhombohedral phases are stable. The pressure dependence of the Néel temperature is ill known ranging from +3.0 to +6.0 K/GPa [3, 5, 6] the pressure dependence of the rhombohedral distortion  $\alpha$  and the magneto-striction  $\delta V/V$  have never been determined as far as we are aware. These pressure coefficients are directly related to the distance-dependence of interatomic exchange parameters, i.e. the microscopic interaction responsible for magnetic order. This issue is of considerable importance because the electronic and magnetic properties of transition metal oxides are very hard to describe by *ab initio* methods and various methods have been proposed to overcome these difficulties, see refs. [7–9] and refs. therein. Due to their simple crystal structure, the 3d-monoxides have traditionally been used to test these methods and it appears hence of importance to provide

accurate experimental data to confront them with.

Here we apply high pressure powder neutron diffraction to investigate MnO across the Néel temperature, to 8.5 GPa, in the temperature range 85-300 K. Compared to other experimental techniques, neutron scattering has the considerable strength of being able to record both crystal and magnetic structure simultaneously, thus allowing to study their mutual interplay with high precision. From the measured shift in  $T_N$ ,  $\alpha$  and  $\delta V/V$  we determine the pressure dependence of nearest and next nearest neighbor exchange constants to second order using analytical relations based on mean field theory. The results are compared to recently published numerical predictions [7, 8] with implications on MnO's phase diagram at much higher pressures.

### EXPERIMENT

Neutron diffraction measurements were carried out at the high-pressure beamline PLANET [10] at MLF, the Japan Proton Accelerator Research Complex (J-PARC), Tokai, Ibaraki, Japan, using double-toroidal sintered diamond anvils [11] with sample volumes of 12 mm<sup>3</sup>, encapsulating TiZr gaskets and a 4:1 methanol-ethanol mixture as pressure transmitting fluid. The sample was purchased from Aldrich (purity 99.99 %) and ground to give a fine powder of less than  $\approx 20$   $\mu$ m particle size. All runs applied a Mito system [12] which allows low temperature measurements to  $\approx 85$  K. The position of the sample was maintained to within  $\pm 0.1$  mm relative to the laboratory frame. A small amount of lead was mixed with the sample and served as a pressure gauge via its accurately known equation of state at variable  $P/T$  conditions [13]. A particular experimental difficulty arises from the fact that the pressure dependence of magnetic

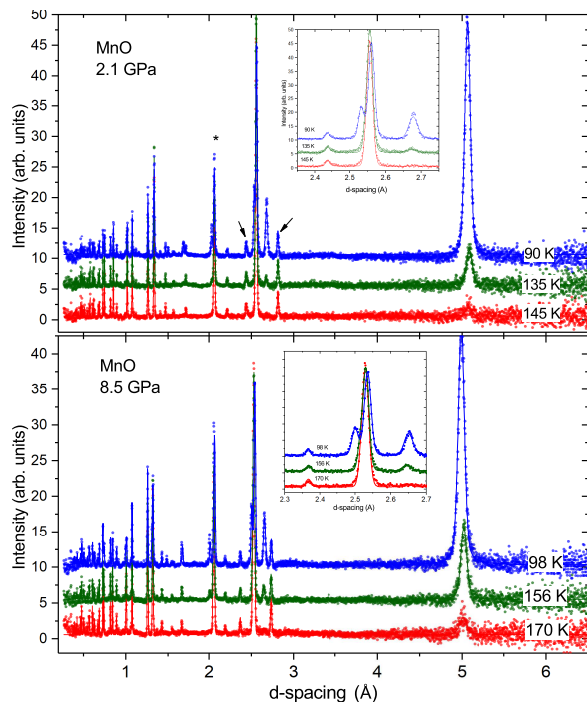


FIG. 1. Neutron diffraction patterns of MnO at 2.1 GPa (top) and 8.5 GPa (bottom) at various temperatures across the Néel temperature. The lines through the data (circles) are fits from Rietveld refinements. The insets give enlarged views over the 2.3-2.8 Å range. Note the splitting of the 111 reflection below the Néel temperature. The asterisks and arrows mark respectively the strongest reflections from diamond (anvils) and lead (pressure marker).

(and probably also structural) properties of MnO appears to be highly sensitive to non-hydrostatic pressure conditions. The pressure dependence of the Néel temperature, for example, is one order of magnitude larger for stress along [111] than under hydrostatic conditions [14]. For this reason, pressure was always changed at room temperature where the 4:1 mixture is in a liquid state. The subsequent cooling under constant load is approximately isochoric and appears to cause no measurable non-hydrostatic stresses. This is demonstrated in Fig. 1 which shows diffraction patterns at low (2.1 GPa) and the highest pressure (8.5 GPa), and various temperatures. Magnetic order is first observable by the appearance of a strong  $1/2 \ 1/2 \ 1/2$  reflection at  $\approx 5$  Å and upon further cooling by a rhombohedral splitting of the 111 nuclear reflection at  $d \approx 2.55$  Å. There is no noticeable broadening of the Bragg reflections across the solidification temperature of the pressure transmitting medium which is approximately 170 K at 2.1 GPa and 265 K at 8.5 GPa [15]: The splitting of the 111 reflection remains sharp even at the highest pressure and lowest temperature, see insets of Fig. 1. From this we conclude that potential non-hydrostatic effects are unobservable. The temperatures were monitored by 3 thermocouples, two of them being

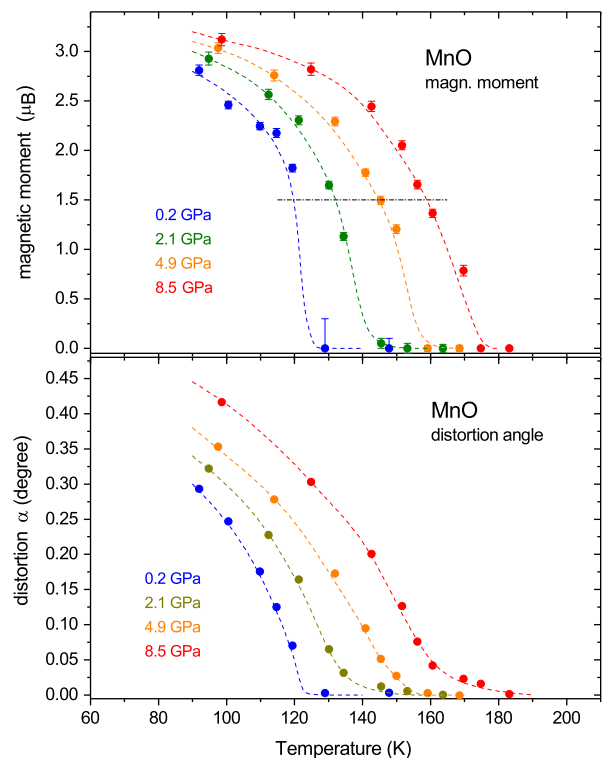


FIG. 2. Magnetic moment (upper) and distortion angle (bottom, defined as positive) of MnO under pressure. The horizontal line in the upper panel indicates  $m=1.5 \mu_B$  (i.e. 1/3rd of the value at 0 K). The lines are guides to the eye.

attached on the steel binding ring of the two anvils and one glued in the hole of the back anvil using Ag-paste, ca. 5 mm from the sample. These confirmed a temperature difference between the two anvils of less than 2 K and an agreement of the three readings of better than 3 K. Given the high thermal conductivity of diamond, the temperature reading from the thermocouple in the back hole is believed to be the most accurate and cited here throughout the text.

Synchrotron x-ray diffraction data were collected at 295 K on the same sample as the neutron measurements. We used a membrane diamond anvil cell with anvils of 300  $\mu\text{m}$  culet, a rhenium gasket provided with a 130  $\mu\text{m}$  hole and neon as pressure transmitting medium. Neon maintains good hydrostatic conditions up to  $\approx 50$  GPa [15], i.e. up to pressures where magnetic long-range order has been reported to occur at room temperature [1, 3]. Pressure values were determined from the refined lattice constants of neon and its equation of state reported by Dewaele et al. [16].

Neutron diffraction patterns were analysed by Rietveld methods using Fullprof [17] refining a minimum of structural and magnetic parameters. The fits included refinements to minority phases from the pressure marker (Pb, space group  $Fm\bar{3}m$ ) and diamond (space group  $Fd\bar{3}m$ )

from the anvils. For the sample, the analysis was carried out in space group  $R\bar{3}m$  (both above and below  $T_N$ ) refining lattice constants, the magnetic moment  $m$ , thermal displacement, profile and absorption parameters. It should be pointed out that high resolution diffraction revealed that the distortion below  $T_N$  is not exactly rhombohedral but results in a monoclinic ground state with most likely space group  $C2/m$  [18]. The resolution of our data (and all high pressure neutron diffraction data published so far) is by far insufficient to resolve this deviation from space group  $R\bar{3}m$ . For this reason it was ignored in our analysis, as it is ignored in all *ab initio* calculations our data will be compared with.

## RESULTS AND DISCUSSION

Figures 2 and 3 give the temperature and pressure dependence of the refined magnetic moment and the rhombohedral distortion defined as the deviation from 90 degree from the equivalent cubic unit cell. With the limited number of data points it is not possible to derive Néel temperatures with high precision. For this reason and the fact that we are only interested in shifts, we define  $T_N$  somewhat arbitrarily as the temperature where the refined magnetic moment reaches  $1.5 \mu_B$ , i.e 1/3rd of the saturation moment ( $\approx 4.5 \mu_B$ ). This gives  $T_N=120$  K at 0.21 GPa, in good agreement with the accepted literature value, and a pressure shift of  $dT_N/dP=+4.5(5)$  K/GPa. Whatever the exact definition of the Néel temperature, it is clear that diffuse magnetic scattering is visible well above  $T_N$ , typically 10-15 K above. This is shown in Fig. 3 which includes the onset temperatures where first signs of intensity around the  $1/2 \ 1/2 \ 1/2$  reflection can be detected. This finding is very similar to the behaviour observed in NiO where diffuse scattering could be observed up to  $1.5 T_N$  [19]. When this onset temperature is compared with the onset temperature of the lattice distortion we find that they are virtually identical (Fig. 3, upper).

As for the pressure dependence of the lattice distortion (Fig. 2, lower) we determine this quantity at an isotherm of 90 K, though a measurement at 0 K would have been more significant. We find an increase under pressure with a coefficient of  $d\alpha/dP=+0.0180(5)$  deg./GPa. There are no other experimental data to be compared with but spin-polarized density functional calculations including generalized-gradient corrections with on-site Coulomb repulsion U (“GGA+U”) by Schrön et al. [8] predict  $d\alpha/dP=+0.0199(5)$  (at 0 K). This is in rather good agreement considering the measurements were carried out at significantly higher temperatures.

Finally, in order to determine the volume striction, i.e. the change in volume caused by magnetic order at  $T=0$  K, we determine the unit cell volume as a function of temperature, at various pressures. For this purpose we added

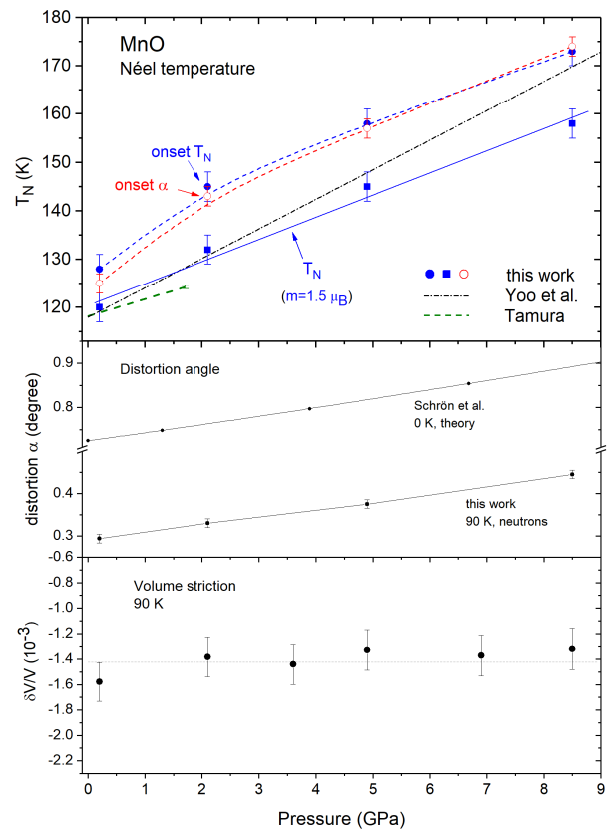


FIG. 3. Pressure dependence of  $T_N$  (upper),  $\alpha$  (middle), and  $\delta V/V$  (lower). The data are compared to experimental findings using a strain gauge technique to 1.7 GPa ( $T_N$  defined as midpoint) [6], x-ray spectroscopy [3], and *ab initio* results by Schrön et al. [8].

data sets from three other runs (at 0.2 GPa, 3.6 GPa and 6.9 GPa) which were carried out with ceramic anvils but where the temperature reading was less accurate, a fact which is less critical in this context. Cooling over such a large temperature range leads to a small drop in pressure (typically less than 0.2 GPa) which was corrected by using the known bulk modulus of MnO ( $B_0=150$  GPa [20]), i.e. the data in Fig. 4 are strictly isobaric. Arrows indicate the respective Néel temperatures (according to the definition given above) and the onset temperature for magnetic diffraction signal. It is obvious that a visible volume change sets in at temperatures well below the point where diffuse scattering appears. In fact a deviation from the  $V(T)$  behaviour in the paramagnetic region can only be seen at temperatures where the moment  $m$  reaches a sizable value, typically  $1.5 \mu_B$ .

The determination of the pressure dependence of the volume striction is less straightforward than that of  $T_N$  and  $\alpha$  and considerably less precise. For this purpose we follow the same strategy as Morosin [21] for the ambient pressure data. We use a Grüneisen approach to describe the thermal expansion above  $T_N$ :

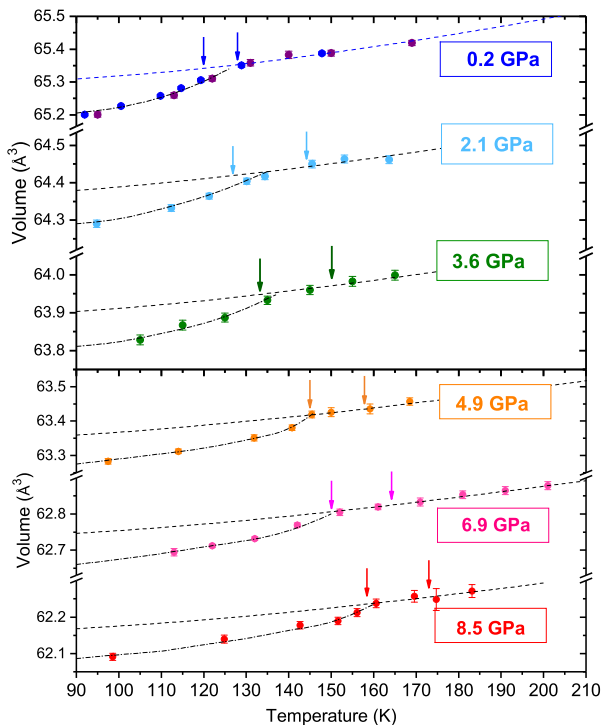


FIG. 4. Temperature dependence of the unit cell volume of MnO at various pressures. The dotted lines below the Néel temperatures are guides to the eye. The dashed lines describes the behaviour in the absence of magnetic order derived from a Grüneisen model as explained in the text. The right and left arrows in each panel indicate temperatures where magnetic signal is first visible and where the refined moment reaches  $1.5 \mu_B$ , respectively.

$$V(T) = V_0 \left( 1 + \frac{AE}{(1 - CE)} \right) \quad (1)$$

where  $V_0$  is the volume at 0 K in the absence of magnetic order,  $E$  is the internal energy related to the Debye function  $D(T, \theta)$  by  $E(T) = 3RTD(T, \theta)$  with  $\theta$  the Debye temperature, and  $A$  and  $C$  are parameters proportional to  $\gamma/VB$  ( $B$  the bulk modulus and  $\gamma$  the Grüneisen parameter). Starting from the published ambient pressure value  $\theta=425$  K [21], we determine the Debye temperatures at 2.1, 3.6, 4.9, 6.9 and 8.5 GPa from the known pressure dependence of the elastic constants  $C_{11}$ ,  $C_{12}$  and  $C_{44}$  [20] using Launey's tables [22]. We obtain 434 K (2.1 GPa), 441 K (3.6 GPa), 447 K (4.9 GPa), 458 K (6.9 GPa), 466 K (8.5 GPa). With the ambient pressure values  $A=3.42 \times 10^{-5} \text{ J}^{-1}$ ,  $C=30.6 \times 10^{-5} \text{ J}^{-1}$  [21] and the pressure dependence of  $\gamma/VB$  derived from the known bulk modulus  $B_0$  and its pressure derivative  $B'_0$ , and taking  $\gamma \propto V^{-1}$  we obtain the dashed lines through the data with  $V_0$  as a fitting parameter. The volume striction is then the difference between this line and the measured data below  $T_N$ . If we take the dotted lines

in Fig. 4 through the data (below  $T_N$ ), we obtain the volume striction at 90 K as shown in Fig. 3, lower panel. The error bars are obviously large but it is clear that the pressure change over 8.5 GPa is rather small, probably close to zero. Since  $(\delta V/V)^{1/3}$  is proportional to the pressure coefficient of  $T_N$  (see eq. 4 further below), we conclude that there cannot be much change in the pressure slope of the Néel temperature. The large pressure dependence of  $dT_N/dP=+6$  K/GPa reported from x-rays measurements up to 30 GPa [3] can therefore not be explained by a potential strong increase in  $dT_N/dP$  under pressure.

Our high-pressure neutron data finally allow conclusions on the pressure (distance) dependence of the interatomic exchange parameters. We recall that numerous investigations have shown that the magnetic properties of MnO can be expressed using a spin Hamiltonian of the form [14, 21, 23]

$$H = -2 \sum_{(i,j)} J_1 S_i S_j - 2 \sum_{(i,j)} J_2 S_i S_j \quad (2)$$

where the first sum runs over the 12 nearest neighbors (6 of them in the same (111) plane, 6 of them in adjacent planes), the second over the 6 next-nearest neighbours, and where  $\mathbf{S}_1(\mathbf{S}_2)$  are spin operators and  $J_1(J_2)$  coupling constants. More sophisticated expressions using bilinear or anisotropy terms were shown to be either unnecessary or only relevant for describing details of the spin wave dispersion [23, 24]. Below  $T_N$  there are strictly speaking two  $J_1$  due to the distortion of the high temperature fcc lattice. We will ignore this detail and assume a single average  $J_1$ , as it is done in all first principle calculations our data will be compared with. The derivatives of  $J_1$  and  $J_2$  with respect to interatomic distances  $r$  are related to the distortion angle  $\alpha$  and the magnetostriction  $\delta a/a$  by the relations [14, 21, 23, 25]

$$\alpha = -\frac{2(N/V)S^2}{C_{44}} \frac{\partial J_1}{\partial \ln r} \quad (3)$$

$$\delta a/a = -\frac{2(N/V)S^2}{(C_{11} + 2C_{12})} \frac{\partial J_2}{\partial \ln r} \quad (4)$$

where  $C_{ij}$  are the cubic elastic constants,  $S=5/2$  and  $r$  the interatomic distances. These relations hold only for  $T=0$  K and temperatures well below  $T_N$ . In addition, in the mean field approximation,  $J_2$  is related to the Néel temperature via

$$T_N = 4k_B S(S+1)J_2 \quad (5)$$

A measurement of the pressure dependence of  $\alpha$ ,  $\delta a/a$  and  $T_N$  allows therefore to derive the dependence of

$J_1$  and  $J_2$  as a function of  $r$  to second order. Starting with the ambient pressure values  $(N/V)=4.6\times 10^{22}$   $\text{cm}^{-3}$ ,  $C_{44} = 78$  GPa,  $S=5/2$ ,  $\alpha=1.1\times 10^{-2}$  at  $T=0$  K gives  $dJ_1/d\ln r = -9.3$  meV using eq. 3, i.e. with  $J_1=5$  K (0.43 meV)  $d\ln J_1/d\ln r = -22$ , as previously reported in Refs. [14, 21, 23, 25]. From the measured pressure dependence  $d\alpha/dP=+0.018$  deg./GPa and taking the derivative of eq. 3 with  $dC_{44}/dp \approx 0$ ,  $B_0=150$  GPa, and  $B'_0 = 5$  [20], we obtain for the second derivatives  $d^2 J_1/d(\ln r)^2 = +92$  meV and  $d^2 J_1/dP^2 = -2.3\times 10^{-4}$  meV/GPa<sup>2</sup>. With these derivatives known we plot in Fig. 5 the normalized [25] pressure dependence of  $J_1$  obtained from our experiment to 8.5 GPa and compare it to first principles calculations by Fischer et al. [7]. The agreement is remarkable.

A similar analysis can be made for  $J_2$ , based on eq. 4, though the large errors in the measured  $\delta a/a(P)$  limits the precision. First, with the ambient pressure values  $\delta a/a=1.1\times 10^{-3}$  (at 0 K),  $C_{11}=230$  GPa and  $C_{12}=117.5$  GPa [20, 21] we find  $dJ_2/d\ln r = -5.6$  meV and hence  $dJ_2/dP = +0.0124$  meV/GPa. We note that this is very close to the value expected from eq. 5 using our measured value for  $dT_N/dP=4.5$  K/GPa, i.e. 0.011 meV/GPa, despite the well-known fact that this mean field formula strongly overestimates the Néel temperature ( $J_2=0.474$  meV would give  $T_N=192.5$  K). For the measured pressure dependence of the volume striction (Fig. 3, lower panel) the most unbiased assumption is  $d(\delta V/V)/dP \approx 0$ . If we admit this value and using again the published pressure dependence of the elastic constants [20] we obtain from eq. 4 the second derivatives  $d^2 J_2/d(\ln r)^2 = +58$  meV and  $d^2 J_2/dP^2 = -1.3\times 10^{-4}$  meV/GPa<sup>2</sup>. This is plotted in Fig. 5 (lower panel) and compared to theory. The agreement is reasonable.

Insight in the behaviour of  $J_2$  over a large pressure range might be gained from x-ray diffraction data recorded at 295 K to 60 GPa as shown in Fig. 6. The rhombohedral distortion is clearly absent up to at least 38.2 GPa and appears first at 42.7 GPa. We conclude that at room temperature and under hydrostatic conditions, long-range order sets in at 42 GPa. This means an average increase of  $T_N$  with a rate of  $dT_N/dP=4.2$  K/GPa which is in excellent agreement with the neutron result of  $dT_N/dP=4.5(5)$  K/GPa based on data to 8.5 GPa. For this reason  $dT_N/dP$  must be approximately constant over 40 GPa, and because of eqs. 5 and 4 also  $dJ_2/dP$  and  $\delta V/V(P)$ . We hence find again that the volume striction is pressure insensitive.

## CONCLUSION

The data presented here highlight the complexity of the magneto-elastic transition in MnO under pressure, and presumably in other 3d-monoxides: Diffuse magnetic scattering appears well above  $T_N$ , approximately 10-20 K

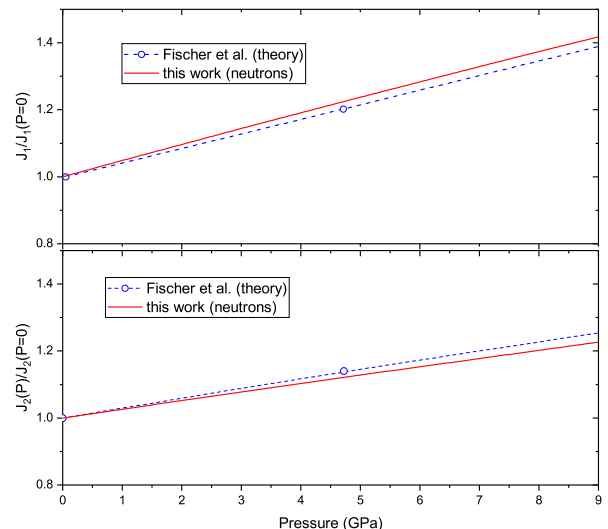


FIG. 5. Pressure dependence of exchange parameter  $J_1$  and  $J_2$  derived from this work (solid lines) and compared to calculations by Fischer et al. [7].

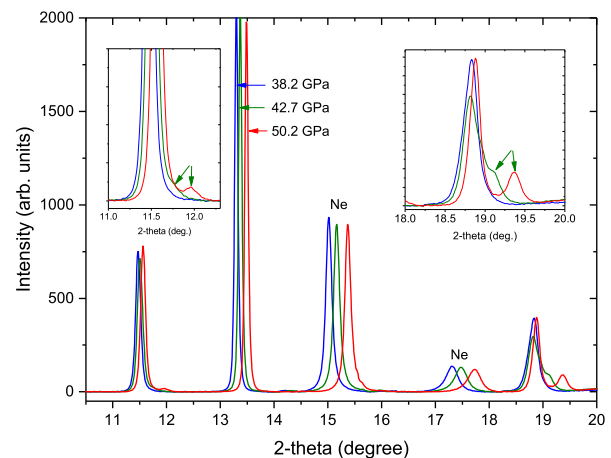


FIG. 6. X-ray diffraction patterns of MnO recorded at 295 K and increasing pressure. Note the progressive splitting (arrows) of the cubic 111 and 220 reflections above 42.7 GPa which signals magnetic ordering. Reflections of solid neon (pressure transmitting medium) are marked.  $\lambda=0.486$  Å.

above, and simultaneously with the onset of a rhombohedral lattice distortion, but with no sign in the  $V(T)$  dependence. Volume striction is seen to set in only when the magnetic moment attains a sizable magnitude, typically  $1.5 \mu_B$ . In how far these observations are due to microstructure effects (polycrystalline nature of the sample) remains to be shown. We find a pressure coefficient  $dT_N/dP=+4.5(5)$  K/GPa, in remarkable agreement between the neutron data and hydrostatic x-ray diffraction measurements to 60 GPa. This value is considerably larger than derived from previous strain-gauge measurements to 0.2 GPa [5] ( $+3.0(2)$  K/GPa) and to 1.6 GPa [6]

(+3.7(2) K/GPa), but significantly smaller than reported x-ray spectroscopy data [3] (+6.0 K/GPa). Although we cannot detect any indication of non-hydrostatic effects, it is impossible to entirely exclude them. If they exist they would *overestimate* the true hydrostatic pressure coefficient due to the extremely strong pressure coefficient along [111] [14], i.e. the value we cite should be regarded as the upper limit. We find the rhombohedral distortion  $\alpha$  to *increase* with pressure with a rate which is very well reproduced by first-principles calculations. In contrast, the volume striction  $\delta V/V$  is found to be insensitive to pressure. X-ray diffraction measurements show that at 295 K, MnO attains long-range magnetic order at 42 GPa, i.e. considerably higher than the previously reported value of 30 GPa [3], but consistent with an extrapolation of our neutron data and predictions of theory [7].

This work was based on experiments performed at the Japanese neutron spallation source MLF under Proposal No. 2018A0276. Neutron diffraction experiments were carried out with a financial support from JSPS (grant no. 18H05224). S.K. acknowledges financial support through the joint CNRS-JSPS grant no. PRC2191, help from P. Parisiadis and Y. Guarnelli in the preparation of the DAC, as well as access to beamtime on the PSICHÉ high pressure beamline of the French synchrotron SOLEIL.

---

\* Corresponding author: Stefan.Klotz@upmc.fr

- [1] T. Kondo, T. Yagi, Y. Syono, Y. Noguchi, T. Atou, T. Kikegawa, and O. Shimomura, *J. Appl. Phys.* **87**, 4153 (2000).
- [2] J.-P. Rueff, A. Mattila, G. Vanko, and A. Shukla, *J. Phys.: Condens. Matter* **17**, S717 (2005).
- [3] C. Yoo, B. Maddox, J.-H. Klepeis, V. Iota, A. McMahan, M. Hu, P. Chow, M. Somayazulu, D. Häusermann, R. Scalettar, and W. Pickett, *Phys. Rev. Lett* **94**, 115502 (2005).
- [4] J. Patterson, C. Aracne, D. Jackson, V. Malba, S. Weir, P. Baker, and Y. Vohra, *Phys. Rev. B* **69**, 220101(R) (2004).
- [5] H. Bartholin, D. Bloch, and R. Georges, *Comptes Rend. Acad. Sci. Paris* **264**, 360 (1967).
- [6] S. Tamura, *High Temperatures - High Pressures* **19**, 657 (1987).
- [7] G. Fischer, M. Däne, A. Ernst, P. Bruno, M. Lüders, Z. Szotek, W. Temmerman, and H. W., *Phys. Rev. B* **80**, 014408 (2009).
- [8] A. Schrön, C. Rödl, and F. Bechstedt, *Phys. Rev. B.* **86**, 115134 (2012).
- [9] J. Kuneš, A. Lukoyanov, V. Anisimov, T. Scalettar, and W. Pickett, *Nature Materials* **7**, 198 (2008).
- [10] T. Hattori *et al.*, *Nucl. Instrum. Meth. Phys. Res. A* **780**, 55 (2015).
- [11] S. Klotz, *Techniques in High Pressure Neutron Scattering*, Taylor and Francis, CRC, Boca Raton (2013).
- [12] K. Komatsu, M. Moriyama, T. Koizumi, K. Nakayama, H. Kagi, J. Abe, and S. Harjo, *High Pressure Research* **33**, 208 (2013).
- [13] T. Strässle, S. Klotz, K. Kunc, V. Pomjakushin, and J. S. White, *Phys. Rev. B* **90**, 014101 (2014).
- [14] D. Bloch and R. Maury, *Phys. Rev. B* **7**, 4883 (1973).
- [15] S. Klotz, L. Paumier, G. Le Marchand, and P. Munsch, *High Pressure Research* **29**, 649 (2009).
- [16] A. Dewaele, F. Datchi, P. Loubeyre, and M. Mezouar, *Phys. Rev. B* **77**, 094106 (2008).
- [17] J. Rodríguez-Carvajal, *Physica B* **192**, 55 (1933).
- [18] S. Lee, Y. Ishikawa, P. Miao, S. Torii, T. Ishigaki, and T. Kamiyama, *Phys. Rev. B* **93**, 064429 (2016).
- [19] T. Chatterji, G. McIntyre, and P.-A. Lindgard, *Phys. Rev. B* **79**, 172403 (2009).
- [20] R. Pacalo and E. Graham, *Phys. Chem. Minerals* **18**, 69 (1991).
- [21] B. Morosin, *Phys. Rev. B* **1**, 236 (1970).
- [22] G. Alers, *Physical Acoustics*, W.P. Mason editor, Academic Press, New York, p. 1-42 (1965).
- [23] M. Lines and E. Jones, *Phys. Rev.* **139**, 1313 (1965).
- [24] G. Pepy, *J. Phys. Chem. Solids* **35**, 433 (1974).
- [25] The various reported values of  $J_1$  ( $J_2$ ) depend on the definition of the Hamiltonian (including the summation convention) and the  $S_1$  ( $S_2$ ). We adopt the definition given in eq. 2 from which eq. 5 can be derived [26], as well as eqs. 3 and 4 [14]. For this reason it is preferable to compare the normalized values and their derivatives, whenever possible.
- [26] J. Callaway, *Quantum Theory of the Solid State*, Academic Press, New York (1974).